PAPER

Check for updates

A low temperature aqueous formate fuel cell using cobalt hexacyanoferrate as a non-noble metal oxidation catalyst†

Lijuan Han,[ab] Jesús González-Cobos, [ID][a] Irene Sánchez-Molina,[a] Stefano Giancola,[a] Scott J. Folkman, [ID][a] S. Giménez,[c] A. Vidal-Ferran [ID][de] and José Ramón Galán-Mascarós [ID] *[ae]

Cobalt hexacyanoferrate, the Co–Fe Prussian blue derivative (CoFePB), is an effective, selective and stable electrocatalyst for formate oxidation, exhibiting robust performance under a variety of electrolyte conditions. In this work, we test CoFePB as a non-noble-metal formate oxidation catalyst in a liquid fuel cell, with formate acting as a carbon-based, water soluble, hydrogen carrier. Herein we fabricate two proof-of-concept aqueous direct formate fuel cells. One uses CoFePB as a formic acid oxidation catalyst coupled with Pt as an oxygen reduction reaction catalyst and delivers a maximum power density of 67 $\mu W\ cm^{-2}$. The second one, based on carbon felt as a cathode and Ce^{4+} as a terminal electron acceptor, shows a stable maximum power output of 8.6 $mW\ cm^{-2}$. This is, to our knowledge, the first example of a noble-metal-free direct formate oxidation fuel cell.

Introduction

The intermittent and diverse nature of renewable energy sources requires the utilization of new vectors to store and deliver energy in an efficient and environmentally friendly manner. Chemical fuels are attractive energy storage systems due to their high energy density and relative ease of storage and transportation.[1,2] Hydrogen and other small molecules, such as formate/formic acid, methanol or methane, can be sustainably obtained from photo/electrochemical transformation of water and carbon dioxide.[3] The stored energy in these small organic molecules can then be extracted *via* oxidation of the products in a fuel cell.[4] Hydrogen fuel cells (HFCs) have been commercially available for decades. Despite their excellent reliability, two major drawbacks remain unsolved in this technology; on one end, hydrogen is a gas under ambient conditions, and is typically stored by liquefaction at low temperatures or by compression under high pressure for greater volumetric energy

density.[5,6] On the other hand, low-temperature hydrogen fuel cells still require precious metal catalysts, *i.e.* platinum-group metals (PGMs), to reach their maximum potential, jeopardizing their wide spread dissemination.[7]

To mitigate the first problem, liquid hydrogen carriers (such as C-based alcohols, acids and sugars) have been proposed as alternative H_2 storage media with higher volumetric energy densities and greater ease of transport, handling and storage.[8–13] The energy stored in the organic molecules is then released either by decomposition *in situ* to deliver hydrogen for HFC use or, more efficiently, through a liquid fuel cell directly oxidizing the organic molecule.[14,15] In the last few years, increasing attention has been focused on direct formate fuel cells (DFFCs).[16,17] DFFCs have indeed higher theoretical cell voltage (1.45 V with oxygen as the oxidant) with respect to other liquid fuel cells running on methanol (1.21 V) or ethanol (1.14 V). Moreover, formate can be easily stored and transported as a salt, thus minimizing hazards. Formate production by CO_2 electrochemical reduction and its direct use in DFFCs have been already reported in a single device also using sunlight as the energy source.[11,13]

Nevertheless, direct and selective oxidation of formate requires the use of electrocatalysts traditionally based on noble metals. Most DFFCs reported use either O_2 or H_2O_2 as an oxidant and employ Pd/C-based anodes and Pt/C-based cathodes, with metal loadings ranging from 2 to 4 $mg\ cm^{-2}$.[16] In addition to the scarcity of Pd and Pt, the use of these metals in formate oxidation is limited by the low tolerance to impurities present in fuels, or poisoning by the adsorbed intermediates (such as CO) during operation, resulting in the rapid decay of catalytic performance

[a]*Institute of Chemical Research of Catalonia (ICIQ), The Barcelona Institute of Science and Technology (BIST), Av. Paisos Catalans, 16, 43007 Tarragona, Spain. E-mail: Jrgalan@iciq.es*

[b]*Departament de Química Física I Inorgánica, Universitat Rovira i Virgili, Marcel.lí Domingo s/n, 43007 Tarragona, Spain*

[c]*Institute of Advanced Materials (INAM), Universitat Jaume I, 12006 Castelló, Spain*

[d]*Departament de Química Inorgànica I Orgànica, Universitat de Barcelona, c/ Martí i Franqués, 1-11, 08028 Barcelona, Spain*

[e]*ICREA, Pg. Lluís Companys 23, 08010 Barcelona, Spain*

and low current densities.[14,18] Much effort must be expended on decreasing the catalyst metal loadings and finding alternatives. One common approach is to employ other transition metals in conjunction with Pd or Pt.[19–21] Some examples of noble-metal-free electrocatalysts for anodic oxidation of small hydrocarbon molecules like methanol ethanol or formic acid have been reported in the literature.[22–27] Interestingly, there is only one publication with a direct formic acid fuel cell, where the anode is made of MnO_2 and polyaniline and the cathode, where the oxygen reduction reaction (ORR) takes place, is Pt/C. This cell had an open circuit potential of 0.55 V and maximum power density of 3 mW cm^{-2} at 10 mA cm^{-2} at room temperature.[28]

We previously studied the cobalt hexacyanoferrate Prussian blue derivative (CoFePB) in the context of water oxidation, where it proved to be a versatile and robust electrocatalyst.[29,30] Recently, we discovered that CoFePB exhibits excellent selectivity and high current density for aqueous $HCOOH/HCOO^-$ oxidation in a wide pH range.[31] Moreover, it is unique when compared to Pt and Pd, in that it is not poisoned by CO or other intermediates at a high current density—indeed CoFePB can achieve current densities > 10× higher than Pt or Pd@C.[31] Herein, we report the implementation of this electrocatalyst in two aqueous formate fuel cells, one based on molecular oxygen as the terminal electron acceptor and the other using Ce^{4+} as the terminal electron acceptor. Appropriate catholyte and anolyte solutions were used to maximize cell voltage in acidic and/or basic conditions. These proof-of-concept fuel cells demonstrate the potential of non-noble-metal catalysts, and especially of CoFePB, for selective electrooxidation of organic small molecules as fuels for carbon-neutral electricity generation.

Experimental

Materials and chemicals

All chemicals used were of analytical reagent grade, and included, ammonium cerium(IV) nitrate $Ce(NH_4)_2(NO_3)_6$ (Acros organics), cobalt(II) nitrate hexahydrate $Co(NO_3)_2 \cdot 6H_2O$ (Aldrich), urea 98% CH_4NO_2 (Aldrich), potassium hexacyanoferrate $K_3Fe(CN)_6$ (Aldrich), 98% formic acid solution (Aldrich), 63–67% nitric acid (Aldrich), and 98% sulfuric acid (Aldrich). All solutions were prepared using 18.2 MΩ cm Milli-Q water. If not specified, all commercially available reagents and solvents were used as received without further purification.

Fluorine-tin-oxide coated glass slides (FTO, 12–14 Ω per square surface resistivity) were purchased from Pilkington NSG TEC 15A, 2.2 mm slides with 80.0–81.5% transmittance. Pt foil (99.95%, 0.1 mm thickness) was purchased from Goodfellow. Carbon felt (5 mm thickness) was supplied by NOBRAN Trade & Service Co Ltd. Nafion® 115 (127 μm thinkness) was purchased from Ion Power.

CoFePB electrode preparation

In a typical synthetic procedure,[29] a thin pink film of CoO_x with a 1 × 1 cm^2 geometric surface area was initially grown on a transparent FTO surface by a hydrothermal method. The CoO_x/FTO sample was subsequently placed in the freshly prepared 800 mg/100 mL $K_3Fe(CN)_6$ aqueous solution and heated at 60 °C for 24 hours. Finally, the CoFePB sample was immersed in concentrated H_2SO_4 solution (pH 1) for more than 4 hours to remove any possible remaining traces of oxide, and then rinsed with MilliQ water. The average CoFePB mass loading on the electrodes is 0.3 mg cm^{-2}.

Three-electrode electrochemical measurements

All electrochemical experiments were conducted with a computer-controlled Bio-Logic VMP3 multichannel potentiostat. Formate oxidation was tested on a CoFePB catalyst at pH 13 under ambient conditions. A standard three-electrode arrangement was used with CoFePB/FTO as the working electrode, Pt mesh as the counter electrode and saturated calomel electrode (SCE) as the reference electrode. All the potentials were referred to NHE by adding +0.241 V to the potential vs. SCE. Quasi-steady-state polarization curves were measured at a sweep rate of 5 mV s^{-1} under magnetic stirring (600 rpm). The formate concentration in the electrolyte solution was 2 M, and 1 M KNO_3 was added to reduce the impact stemming from mass diffusion and to ensure good ionic conductivity. The pH was adjusted by adding aliquots of concentrated KOH or HNO_3.

Fuel cell tests

Fuel cell measurements were conducted in a H-shaped cell with a Nafion® 115 membrane (127 μm thick) as the separator, a CoFePB/FTO (catalyst loading 0.3 mg cm^{-2}) electrode as the anode; and Pt foil (1.5 cm × 1.5 cm) or carbon felt (1 cm × 1 cm^2) as the cathode. First a formate/oxygen fuel cell (FC1) was tested where the anolyte was 2 M $HCOO^-$ solution (pH 13), prepared as mentioned above, and the catholyte was 1 M H_2SO_4 solution (pH 0), saturated with oxygen by air bubbling. Then a formate/Ce^{4+} fuel cell (FC2) was tested where the anolyte was a 2 M $HCOO^-$ solution (pH 13) and the catholyte was 1 M $Ce(NH_4)_2(NO_3)_6$ in 1 M HNO_3 solution (pH 0). Polarization curves were collected at 25 or 60 °C. The potential range spans from the open circuit potential to 0.1 V, and each point was collected when the steady state was reached (after ca. 5–10 min). Both the sides are under ambient pressure as well as under magnetic stirring (600 rpm). For the durability test, the glass cell was connected to two glass reservoirs (1 L each) for the anode and cathode solutions. Each electrolyte was continuously fed into the cell with a flow of 50 mL min^{-1} through two peristaltic pumps (Verderflex EV500). The fuel cell scheme can be observed in Fig. S1 of the ESI.†

Results and discussion

Electrochemical behaviour

We recently reported details of formate electrooxidation using CoFePB as a heterogeneous electrocatalyst under various conditions.[31] The key points are that (i) we characterized CoFePB electrochemical properties and stability using cyclic voltammetry (CV), electrochemical impedance spectroscopy (EIS), and chronoamperometry. Furthermore, (ii) CoFePB was studied before and after prolonged electrolysis using SEM, IR

and Raman no significant structural changes were observed and (iii) comparison with heterogeneous CoO_x confirms that CoFePB is the true electrocatalyst and that it exhibits robust stability in the experimental time frames studied.[24] Lastly, (iv) CoFePB is not poisoned by intermediates of formate oxidation and therefore is able to achieve much higher current density than Pt and Pd.

For the present work, formate electrooxidation on CoFePB was first studied in the half-cell configuration by using pH 13 with 2 M formate and 1 M KNO_3, since these conditions ensure the lowest onset potential of formate oxidation. Fig. 1 shows the cyclic voltammogram (CV) obtained with the CoFePB electrode with 2 M formate, and under identical conditions without added formate. A large, irreversible anodic current is observed at potentials >+0.35 V $vs.$ NHE in the presence of formate that is not observed in the pH 13 electrolyte alone. In other studies with Pd[32–34] or Pt[35–37] catalysts several oxidation peaks are instead observed in both forward and reverse scans. These peaks are ascribed to the direct formate oxidation followed by formation of Pd or Pt oxide layers and/or adsorption of poisoning intermediate species (in the forward scan) and to the further oxidation of these reaction intermediates, known as indirect formate oxidation (in the reverse scan). In contrast, herein the expected Co^{II}/Co^{III} redox couple (at $ca.$ 0.4 V $vs.$ NHE at pH 13)[29] is hidden by the formate oxidation wave and does not lead to any catalyst deactivation at high potentials. The apparent absence of hysteresis between positive and negative scans indicates a negligible inhibition rate or a low tendency towards surface poisoning under these conditions, in contrast with Pt-based electrocatalysts, which show severe poisoning by CO adsorbed species.[16,31]

Fuel cell performance

The high selectivity and poison resistance shown by the CoFePB electrocatalyst open prospects for its use in a low temperature aqueous fuel cell. Oxygen is a preferred oxidant for fuel cells,
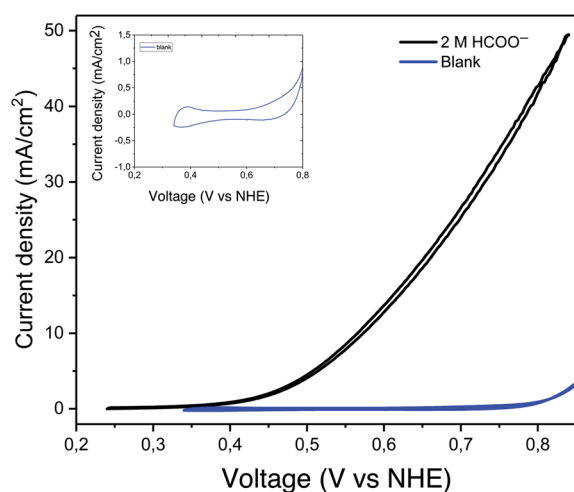
being readily available, with a standard oxidation potential of 1.23 V at pH 0. Theoretically, this thermodynamic potential should be enough to use O_2 as an oxidant in a formate fuel cell with a CoFePB anode, with an onset potential for formate oxidation of $ca.$ +0.35 V at pH 13. Thus, the use of electrolyte solutions with pH 0 and 13 for the catholyte and anolyte, respectively, could lead to the achievement of a cell voltage of up to 0.88 V.

The first electrochemical cell (FC1) consisted of an anode side based on the CoFePB/FTO electrode immersed in a 2 M formate solution (pH 13) and a cathode side with a Pt foil electrode immersed into a O_2-saturated 1 M H_2SO_4 solution (pH 0). Pt has been selected as it is the benchmark catalyst for the oxygen reduction reaction (ORR)[38–40] and is commonly used in DFFCs.[16,17] To hold the pH difference between the cathode and the anode sides, the two half-cells were separated by a Nafion® 115 membrane. A Nafion® ionomer is generally employed as proton exchange membrane in acid media fuel cells, however it has also been applied as a cation exchange membrane in DFFCs to separate a basic anode from an acid cathode.[41–43] The capacity of this membrane to effectively separate the two compartments was confirmed by measuring both catholyte and anolyte pH, which proved to be stable in all experiments (2–3 hours each). Fig. 2 shows the V $vs.$ J curve and the related power density of the FC1 fuel cell.

This fuel cell shows a commonly shaped J–V curve with an open circuit voltage (OCV) of $ca.$ 0.5 V and a maximum power density of 67 $\mu W\ cm^{-2}$ at 0.18 V and 372 $\mu A\ cm^{-2}$ which is in the same range as other formate/oxygen biofuel cells using non-PGM anodes.[44,45] The obtained power density is even lower in the case of a similar fuel cell configuration but employing Pt foil as the anode (30 $\mu W\ cm^{-2}$, see Fig. S2†), likely influenced by the poisoning effect mentioned above. The low performance of this fuel cell device can be explained by the high overpotentials required for both the formate oxidation and the ORR. In fact, the best ORR catalysts need >280 mV overpotential to reach very low currents in liquid electrolyte.[46,47] In the case of formate oxidation, the onset overpotential required with the CoFePB
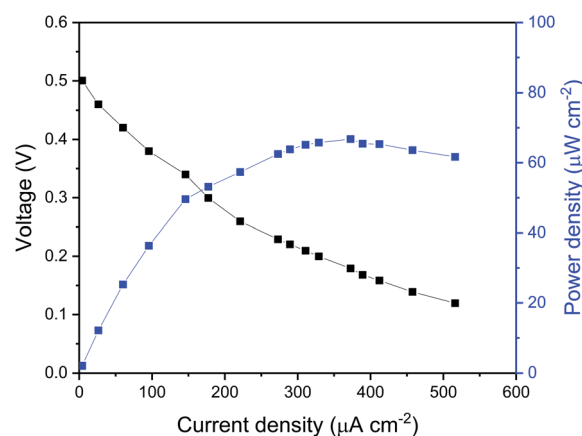

Fig. 1 Cyclic voltammograms (CV) on the CoFePB electrode with pH 13 electrolyte (1 M KNO_3) in the presence (black) and in the absence (blue) of formate. Scan rate of 5 mV s^{-1}. The inset shows the Co^{II}/Co^{III} redox peak at around 0.4 V $vs.$ NHE.

Fig. 2 Polarization curve and power density of the formate/oxygen fuel cell FC1 at 25 °C. Anode: CoFePB/FTO; anolyte: 2 M $HCOO^-$ (pH 13); cathode: Pt foil; catholyte: 1 M H_2SO_4 (pH 0).

catalyst has been estimated[48] as *ca.* 1.32 V. This value was obtained by considering the onset formate oxidation potential empirically obtained in Fig. 1 (*ca.* +0.35 V *vs.* NHE at pH 13) and a theoretical oxidation potential of -0.97 V at pH 13. The latter value was calculated from a standard formic acid/formate oxidation potential of -0.20 V, taken from the literature (this value varies from -0.17 to 0.25 V depending on the precise conditions).[16,20,49–52]

In order to overcome these issues, we fabricated another fuel cell, FC2, where oxygen was replaced by Ce^{4+} as the oxidant with a standard potential of 1.61 V *vs.* NHE.[53–55] The reduction of Ce^{4+} does not exhibit complications such as side reactions, bubbles, disproportionation, or poisoning, and can be reduced on carbon electrodes. To determine the best electrode for Ce^{4+} reduction, a series of materials were evaluated by linear sweep voltammetry, including carbon felt, FTO, Au, and Pt (Fig. S3†). The electrochemical reaction on the carbon felt electrode showed the best performance with an onset potential as high as *ca.* 1.5 V *vs.* NHE at pH 0. In this configuration, Ce^{4+} will be reduced to Ce^{3+} at the carbon felt and $HCOO^-$ will be oxidized to CO_2 at the CoFePB surface, with the flow of electrons between anode and cathode resulting in net electrical energy. *J vs. V* curves and the related current density at both 25 °C and 60 °C are reported in Fig. 3.

At 25 °C, an OCV of 1.45 V was obtained with a maximum power density of 5.5 mW cm^{-2} at 11 mA cm^{-2} and 0.45 V. As expected, the use of a stronger oxidant afforded a better fuel cell performance. Similar to the previous fuel cell, no pH variation of the anodic or cathodic solutions was observed during the experiment. This further demonstrates the effectiveness of the Nafion® membrane to separate the two half-cells. Moreover, the colours of both anode and cathode remained unchanged throughout the whole experiment (see Fig. S1†). This visual evidence, in addition to the pH values, measured before and after the catalysis, confirm negligible chemical crossover between the two compartments.
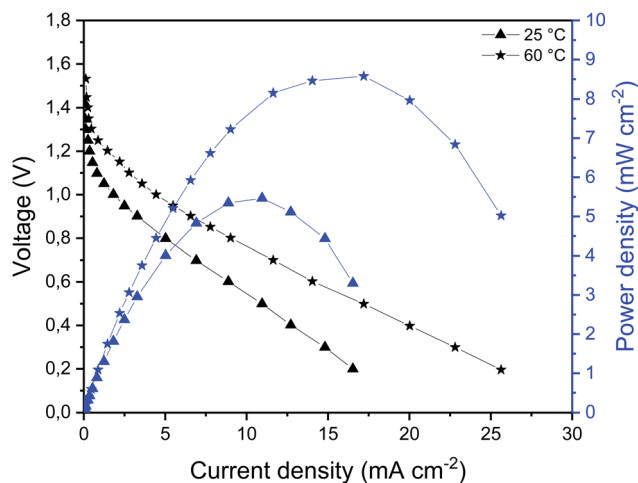
At 60 °C an OCV of 1.52 V was observed while the maximum power density was 8.6 mW cm^{-2} at 17 mA cm^{-2} and 0.5 V. The enhanced fuel cell power output with the increased temperature could be ascribed to the enhanced reaction kinetics at both electrodes and the lower ohmic drop due to the higher ion conductivity of the Nafion® membrane. Similar behaviour has been already reported in other DFFCs.[42,56]

Finally, we developed a set-up, analogous to FC2, working under a continuous supply of reactants (*i.e.* using peristaltic pumps to supply fresh solution), in order to demonstrate the reliability of our device under operating conditions closer to those of actual fuel cells. The polarization curve and the related power density obtained at 60 °C are reported in Fig. 4a.

For this device, a maximum power density of 8.6 mW cm^{-2} was obtained at 0.6 V and 14.4 mA cm^{-2}. These values are similar to those observed in the absence of continuous flow of catholyte and anolyte (Fig. 3), and significantly superior to previous aqueous non-PGM formate fuel cells, typically based on biocatalysts.[44,45] Moreover, in this formate/Ce^{4+} fuel cell configuration, the CoFePB catalyst shows a better performance, in terms of open circuit voltage and maximum current density,
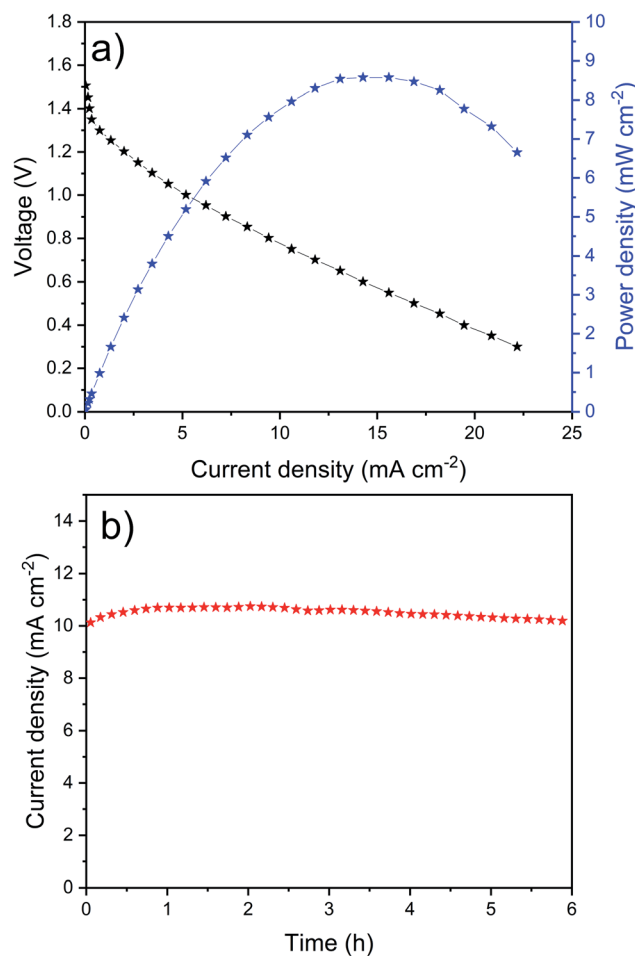

Fig. 4 (a) Polarization curve and power density profile, and (b) chronoamperometry at 0.8 V obtained with the formate/Ce^{4+} fuel cell FC2 at 60 °C under continuous flow of catholyte and anolyte.

Fig. 3 Polarization curve and power density of the formate/Ce^{4+} fuel cell FC2 at 25 °C and 60 °C. Anode: CoFePB/FTO; anolyte: 2 M $HCOO^-$ (pH 13); cathode: carbon felt; catholyte: 1 M Ce^{4+} in 1 M HNO_3 (pH 0).

Table 1   Comparison of electrocatalytic activity of direct formic acid/formate fuel cells using non-PGM anodes

Anode	Cathode	Fuel/oxidant	Fuel cell configuration	$T/°C$	OCV/V	Maximum power density/mW cm^{-2}
PANI/MnO$_2$ (ref. 28)	Pt/C	0.5 M HCOOH + 0.5 M H$_2$SO$_4$/O$_2$	Membrane-electrode assembly	30	0.55	3
				60	0.55	5
CoFePB/FTO	Pt	2 M HCOO$^-$ + KOH (pH 13)/air in 1 M H$_2$SO$_4$ (pH 0)	H-type cell with Nafion® 115 membrane (FC1)	25	0.5	0.07
CoFePB/FTO	Carbon felt	2 M HCOO$^-$ + KOH (pH 13)/1 M Ce^{4+} in 1 M HNO$_3$ (pH 0)	H-type cell with Nafion® 115 membrane (FC2)	25	1.45	5.5
				60	1.52	8.6

as compared with the only direct formic acid fuel cell found in the literature based on a non-PGM anode, PANI/MnO$_2$, in addition, in the Membrane-Electrode Assembly (MEA) configuration.[28] Since in this case a Pt/C cathode was used for the ORR, the proposed formate/Ce^{4+} fuel cell employing carbon felt as the cathode is the first fully PGM-free formate fuel cell. Table 1 compares the performance of these fuel cells.

The maximum power density value obtained herein is still lower than the best-performing oxygen- and hydrogen peroxide-driven formate fuel cells,[16] but in the present study the electrode engineering is yet to be enhanced (thus lowering the formate oxidation overpotentials) and a non-optimized reactor configuration (H-type cell) was employed as a proof of concept, while the state-of-the-art DFFCs consist of MEA configurations. The obtained power output is very promising taking into account the absence of precious metals, the non-optimized anode catalyst amount (over 5 times lower than that generally used in DFFCs[16]), and the very high resistance (ca. 30 Ω) of our liquid electrolyte configuration; especially if compared to MEA configurations, that usually show ohmic drops close to 10^{-2} Ω.

In order to have preliminary evidence of the stability of our fuel cells, chronoamperometry at 0.8 V was performed (Fig. 4b). In this case, the obtained current (10.5 mA cm^{-2}) remained practically constant during the whole experiment (6 hours), which reflects a promising electrochemical stability of our catalyst, its selectivity towards formate oxidation and its high resistance to poisoning with respect to noble metals like Pt and Pd. However, longer accelerated stress tests (for days) should be carried out when implementing the proposed catalyst in a MEA-based device in order to prove the durability of our fuel cell under actual operating conditions.

Conclusions

In this manuscript, we report two proof-of-concept direct formate fuel cells based on a cobalt hexacyanoferrate Prussian blue derivative (CoFePB) as an efficient, selective and stable non-noble-metal catalyst for formate oxidation. The first fuel cell, using Pt as the cathode and saturated oxygen as the oxidant reaches a maximum power density of 67 μW cm^{-2} at 25 °C. The second device, based on a carbon felt cathode and Ce^{4+} as the oxidant showed a maximum power output of 5.5 mW cm^{-2} and 8.6 mW cm^{-2} at 25 °C and 60 °C, respectively. Moreover, stable power generation was obtained for at least 6 hours. This fuel cell is, to the best of our knowledge, one of the first completely

noble-metal-free direct formate fuel cells. Compared to the only other example we could find in the literature, our fuel cell achieves a higher OCV and almost double the power output. Our formate/Ce^{4+} fuel cell shows outstanding performance considering the low loading of CoFePB (0.3 mg cm^{-2}) used and the high resistance (30 Ω) of the fuel cell configuration. This reflects the exceptional activity and selectivity of CoFePB towards formate oxidation and its high resistance to poisoning. Optimization of fuel cell parameters such as type and thickness of the ion exchange membrane and the reactant concentration (especially oxygen) are expected to lead to better device performance, and could pave the way for incorporation of the proposed CoFePB catalyst into other configurations, such as a membrane electrode assembly based fuel cell.

Conflicts of interest

There are no conflicts to declare.

Acknowledgements

References

1   S. Chu, Y. Cui and N. Liu, The path towards sustainable energy, Nat. Mater., 2016, **16**, 16–22.

2   Z. W. She, J. Kibsgaard, C. F. Dickens, I. Chorkendorff, J. K. Nørskov and T. F. Jaramillo, Combining theory and experiment in electrocatalysis: Insights into materials design, Science, 2017, **355**, eaad4998.

3   J. A. Herron, J. Kim, A. A. Upadhye, G. W. Huber and C. T. Maravelias, A general framework for the assessment of solar fuel technologies, Energy Environ. Sci., 2015, **8**, 126–157.

4   W. Vielstich, A. Lamm and H. A. Gasteiger, Handbook of Fuel Cells, Fundamentals Technology and Applications, Wiley-Blackwell, 2003.

5 P. Preuster, A. Alekseev and P. Wasserscheid, Hydrogen Storage Technologies for Future Energy Systems, *Annu. Rev. Chem. Biomol. Eng.*, 2017, **8**, 445–471.

6 U. Bossel, Does a Hydrogen Economy Make Sense?, *Proc. IEEE*, 2006, **94**, 1826–1836.

7 B. C. H. Steele and A. Heinzel, Materials for fuel-cell technologies, *Nature*, 2001, **414**, 345–352.

8 A. F. Dalebrook, W. Gan, M. Grasemann, S. Moret and G. Laurenczy, Hydrogen storage: beyond conventional methods, *Chem. Commun.*, 2013, **49**, 8735–8751.

9 M. Yadav and Q. Xu, Liquid-phase chemical hydrogen storage materials, *Energy Environ. Sci.*, 2012, **5**, 9698–9725.

10 W. H. Wang, Y. Himeda, J. T. Muckerman, G. F. Manbeck and E. Fujita, CO_2 Hydrogenation to Formate and Methanol as an Alternative to Photo- and Electrochemical CO_2 Reduction, *Chem. Rev.*, 2015, **115**, 12936–12973.

11 T. Vo, K. Purohit, C. Nguyen, B. Biggs, S. Mayoral and J. L. Haan, Formate: an Energy Storage and Transport Bridge between Carbon Dioxide and a Formate Fuel Cell in a Single Device, *ChemSusChem*, 2015, **8**, 3853–3858.

12 K. M. Waldie, F. M. Brunner and C. P. Kubiak, Transition Metal Hydride Catalysts for Sustainable Interconversion of CO_2 and Formate: Thermodynamic and Mechanistic Considerations, *ACS Sustainable Chem. Eng.*, 2018, **6**, 6841–6848.

13 X. Lu, Y. Wu, X. Yuan and H. Wang, An Integrated CO_2 Electrolyzer and Formate Fuel Cell Enabled by a Reversibly Restructuring Pb–Pd Bimetallic Catalyst, *Angew. Chem., Int. Ed.*, 2019, **58**, 4031–4035.

14 G. L. Soloveichik, Liquid fuel cells, *Beilstein J. Nanotechnol.*, 2014, **5**, 1399–1418.

15 B. C. Ong, S. K. Kamarudin and S. Basri, Direct liquid fuel cells: A review, *Int. J. Hydrogen Energy*, 2017, **42**, 10142–10157.

16 L. An and R. Chen, Direct formate fuel cells: A review, *J. Power Sources*, 2016, **320**, 127–139.

17 H. Hwang, S. Hong, J. W. Kim and J. Lee, Optimized electrode structure for performance and mechanical stability in a direct formate fuel cell using cation ionomer, *Sustainable Energy Fuels*, 2020, **4**, 1899–1907.

18 E. Antolini, Palladium in fuel cell catalysis, *Energy Environ. Sci.*, 2009, **2**, 915–931.

19 N. Kakati, J. Maiti, S. H. Lee, S. H. Jee, B. Viswanathan and Y. S. Yoon, Anode Catalysts for Direct Methanol Fuel Cells in Acidic Media: Do We Have Any Alternative for Pt or Pt–Ru?, *Chem. Rev.*, 2014, **114**, 12397–12429.

20 A. K. Singh, S. Singh and A. Kumar, Hydrogen energy future with formic acid: a renewable chemical hydrogen storage system, *Catal. Sci. Technol.*, 2016, **6**, 12–40.

21 Y. Pei, Y. Cheng, J. Chen, W. Smith, P. Dong, P. M. Ajayan, M. Ye and J. Shen, Recent developments of transition metal phosphides as catalysts in the energy conversion field, *J. Mater. Chem. A*, 2018, **6**, 23220–23243.

22 S. Rezaee and S. Shahrokhian, Facile synthesis of petal-like NiCo/NiO-CoO/nanoporous carbon composite based on mixed-metallic MOFs and their application for electrocatalytic oxidation of methanol, *Appl. Catal., B*, 2019, **244**, 802–813.

23 D. Wu, W. Zhang and D. Cheng, Facile Synthesis of Cu/NiCu Electrocatalysts Integrating Alloy, Core–Shell, and One-Dimensional Structures for Efficient Methanol Oxidation Reaction, *ACS Appl. Mater. Interfaces*, 2017, **9**, 19843–19851.

24 Z. Jia, Y. Wang and T. Qi, Hierarchical Ni–Fe layered double hydroxide/MnO_2 sphere architecture as an efficient noble metal-free electrocatalyst for ethanol electro-oxidation in alkaline solution, *RSC Adv.*, 2015, **5**, 83314–83319.

25 A. Bisht, P. Pentyala, P. A. Deshpande and S. Sharma, $La_{0.80}Sr_{0.20}CoO_3$ as a noble-metal-free catalyst for the direct oxidation of formic acid under zero applied potential, *Electrochem. Commun.*, 2019, **99**, 1–4.

26 A. Kumar, A. C. Pandey and R. Prakash, Electro-oxidation of formic acid using polyindole-SnO_2 nanocomposite, *Catal. Sci. Technol.*, 2012, **2**, 2533–2538.

27 M. Rosenbaum, F. Zhao, M. Quaas, H. Wulff, U. Schröder and F. Scholz, Evaluation of catalytic properties of tungsten carbide for the anode of microbial fuel cells, *Appl. Catal., B*, 2007, **74**, 261–270.

28 G. K. S. Prakash, P. Suresh, F. Viva and G. A. Olah, Novel single step electrochemical route to γ-MnO_2 nanoparticle-coated polyaniline nanofibers: Thermal stability and formic acid oxidation on the resulting nanocomposites, *J. Power Sources*, 2008, **181**, 79–84.

29 L. Han, P. Tang, Á. Reyes-Carmona, B. Rodríguez-García, M. Torréns, J. R. Morante, J. Arbiol and J. R. Galan-Mascaros, Enhanced Activity and Acid pH Stability of Prussian Blue-type Oxygen Evolution Electrocatalysts Processed by Chemical Etching, *J. Am. Chem. Soc.*, 2016, **138**, 16037–16045.

30 B. Rodríguez-García, Á. Reyes-Carmona, I. Jiménez-Morales, M. Blasco-Ahicart, S. Cavaliere, M. Dupont, D. Jones, J. Rozière, J. R. Galán-Mascarós and F. Jaouen, Cobalt hexacyanoferrate supported on Sb-doped SnO_2 as a non-noble catalyst for oxygen evolution in acidic medium, *Sustainable Energy Fuels*, 2018, **2**, 589–597.

31 L. Han, J. González-Cobos, I. Sánchez-Molina, S. Giancola, S. J. Folkman, P. Tang, M. Heggen, R. E. Dunin-Borkowski, J. Arbiol, S. Giménez and J. R. Galán mascarós, Cobalt Hexacyanoferrate as a Selective and High Current Density Formate Oxidation Electrocatalyst, *ACS Appl. Energy Mater.*, 2020, **3**, 9198–9207.

32 T. Takamura and F. Mochimaru, Adsorption and oxidation of formate on palladium in alkaline solution, *Electrochim. Acta*, 1969, **14**, 111–119.

33 V. Galvan, D. E. Glass, A. F. Baxter and G. K. Surya Prakash, Reduced Graphene Oxide Supported Palladium Nanoparticles for Enhanced Electrocatalytic Activity toward Formate Electrooxidation in an Alkaline Medium, *ACS Appl. Energy Mater.*, 2019, **2**, 7104–7111.

34 S. Sankar, G. M. Anilkumar, T. Tamaki and T. Yamaguchi, Cobalt-Modified Palladium Bimetallic Catalyst: A Multifunctional Electrocatalyst with Enhanced Efficiency and Stability toward the Oxidation of Ethanol and Formate

in Alkaline Medium, *ACS Appl. Energy Mater.*, 2018, **1**, 4140–4149.

35 A. Cuesta, G. Cabello, M. Osawa and C. Gutiérrez, Mechanism of the Electrocatalytic Oxidation of Formic Acid on Metals, *ACS Catal.*, 2012, **2**, 728–738.

36 S.-H. Han, H.-M. Liu, J. Bai, X. L. Tian, B. Y. Xia, J.-H. Zeng, J.-X. Jiang and Y. Chen, Platinum-Silver Alloy Nanoballoon Nanoassemblies with Super Catalytic Activity for the Formate Electrooxidation, *ACS Appl. Energy Mater.*, 2018, **1**, 1252–1258.

37 J. Jiang, J. Scott and A. Wieckowski, Direct evidence of a triple-path mechanism of formate electrooxidation on Pt black in alkaline media at varying temperature. Part I: The electrochemical studies, *Electrochim. Acta*, 2013, **104**, 124–133.

38 M. Liu, L. Wang, K. Zhao, S. Shi, Q. Shao, L. Zhang, X. Sun, Y. Zhao and J. Zhang, Atomically dispersed metal catalysts for the oxygen reduction reaction: synthesis, characterization, reaction mechanisms and electrochemical energy applications, *Energy Environ. Sci.*, 2019, **12**, 2890–2923.

39 K. Singh, E. B. Tetteh, H. Y. Lee, T. H. Kang and J. S. Yu, Tailor-Made Pt Catalysts with Improved Oxygen Reduction Reaction Stability/Durability, *ACS Catal.*, 2019, **9**, 8622–8645.

40 S. Strbac, The effect of pH on oxygen and hydrogen peroxide reduction on polycrystalline Pt electrode, *Electrochim. Acta*, 2011, **56**, 1597–1604.

41 Y. Li, Y. Feng, X. Sun and Y. He, A Sodium-Ion-Conducting Direct Formate Fuel Cell: Generating Electricity and Producing Base, *Angew. Chem., Int. Ed.*, 2017, **56**, 5734–5737.

42 Y. Li, H. Wu, Y. He, Y. Liu and L. Jin, Performance of direct formate-peroxide fuel cells, *J. Power Sources*, 2015, **287**, 75–80.

43 S. G. Silva, J. C. M. Silva, G. S. Buzzo, E. V Spinacé, A. O. Neto and M. H. M. T. Assumpção, PdAu/C Electrocatalysts as Anodes for Direct Formate Fuel Cell, *Electrocatalysis*, 2015, **6**, 442–446.

44 P. Gai, Y. Ji, Y. Chen, C. Zhu, J. Zhang and J. J. Zhu, A nitrogen-doped graphene/gold nanoparticle/formate dehydrogenase bioanode for high power output membrane-less formic acid/O_2 biofuel cells, *Analyst*, 2015, **140**, 1822–1826.

45 S. Sahin, R. Cai, R. D. Milton, S. Abdellaoui, F. C. Macazo and S. D. Minteer, Molybdenum-Dependent Formate Dehydrogenase for Formate Bioelectrocatalysis in a Formate/O_2 Enzymatic Fuel Cell, *J. Electrochem. Soc.*, 2018, **165**, H109–H113.

46 M. Shao, Q. Chang, J. P. Dodelet and R. Chenitz, Recent Advances in Electrocatalysts for Oxygen Reduction Reaction, *Chem. Rev.*, 2016, **116**, 3594–3657.

47 A. Kulkarni, S. Siahrostami, A. Patel and J. K. Nørskov, Understanding Catalytic Activity Trends in the Oxygen Reduction Reaction, *Chem. Rev.*, 2018, **118**, 2302–2312.

48 A. M. Appel and M. L. Helm, Determining the Overpotential for a Molecular Electrocatalyst, *ACS Catal.*, 2014, **4**, 630–633.

49 X. Z. Yuan and H. Wang, PEM Fuel Cell Fundamentals, in *PEM Fuel Cell Electrocatalysts and Catalyst Layers*, ed. J. Zhang, Springer, London, 2008.

50 P. Ferrin, A. U. Nilekar, J. Greeley, M. Mavrikakis and J. Rossmeisl, Reactivity descriptors for direct methanol fuel cell anode catalysts, *Surf. Sci.*, 2008, **602**, 3424–3431.

51 S. Z. Rejal, M. S. Masdar and S. K. Kamarudin, A parametric study of the direct formic acid fuel cell (DFAFC) performance and fuel crossover, *Int. J. Hydrogen Energy*, 2014, **39**, 10267–10274.

52 X. Yu and P. G. Pickup, Recent advances in direct formic acid fuel cells (DFAFC), *J. Power Sources*, 2008, **182**, 124–132.

53 V. Nair and A. Deepthi, Cerium(IV) Ammonium Nitrate – A Versatile Single-Electron Oxidant, *Chem. Rev.*, 2007, **107**, 1862–1891.

54 D. A. Finkelstein, J. D. Kirtland, N. Da Mota, A. D. Stroock and H. D. Abruña, Alternative Oxidants for High-Power Fuel Cells Studied by Rotating Disk Electrode (RDE) Voltammetry at Pt, Au, and Glassy Carbon Electrodes, *J. Phys. Chem. C*, 2011, **115**, 6073–6084.

55 N. Da Mota, D. A. Finkelstein, J. D. Kirtland, C. A. Rodriguez, A. D. Stroock and H. D. Abruña, Membraneless, Room-Temperature, Direct Borohydride/Cerium Fuel Cell with Power Density of Over 0.25 W/cm^2, *J. Am. Chem. Soc.*, 2012, **134**, 6076–6079.

56 T. Q. Nguyen, A. M. Bartrom, K. Tran and J. L. Haan, Operation of the Alkaline Direct Formate Fuel Cell in the Absence of Added Hydroxide, *Fuel Cells*, 2013, **13**, 922–926.